RESEARCH ARTICLE



Check for updates



Upcycling waste PMMA to durable composites via a transesterification-inverse vulcanization process

Shalini K. Wijeyatunga¹ | Katelyn M. Derr¹ | Charini P. Maladeniya¹ | Perla Y. Sauceda-Oloño¹ | Andrew G. Tennyson^{1,2} | Rhett C. Smith¹

Correspondence

Rhett C. Smith, Department of Chemistry, Clemson University, Clemson, SC, 29634, USA.

Email: rhett@clemson.edu

Funding information

National Science Foundation, Grant/Award Number: CHE-2203669

Abstract

Poly(methyl methacrylate) (PMMA) is an important commodity polymer having a wide range of applications. Currently, only about 10% of PMMA is recycled. Herein, a simple two-stage process for the chemical upcycling of PMMA is discussed. In this method PMMA is modified by transesterification with a bioderived, olefin-bearing terpenoid, geraniol. In the second stage, olefinderivatized PMMA is reacted with sulfur to form a network composite by an inverse vulcanization mechanism. Inverse vulcanization of PGMA with elemental sulfur (90 wt.%) yielded the durable composite PGMA-S. This composite was characterized by NMR spectrometry, IR spectroscopy, elemental analysis, thermogravimetric analysis, and differential scanning calorimetry. Composite water uptake, compressional strength analysis, flexural strength analysis, tensile strength analysis, and thermal recyclability are presented with comparison to current commercial structural materials. PGMA-S exhibits a similar compressive strength (17.5 MPa) to that of Portland cement. PGMA-S demonstrates an impressive flexural strength of 4.76 MPa which exceeds the flexural strength (>3 MPa) of many commercial ordinary Portland cements. This study provides a way to upcycle waste PMMA through combination with a naturally-occurring olefin and industrial waste sulfur to yield composites having mechanical properties competitive with ecologically detrimental legacy building materials.

KEYWORDS

chemical recycling, inverse vulcanization, plastic waste, PMMA, terpenes, thiocracking

1 | INTRODUCTION

Poly(methyl methacrylate) (PMMA) is characterized by excellent transparency, high impact resistance, and ease of processing. Its unique physical and chemical properties have led to its widespread utilization in various applications. PMMA's impact resistance and outstanding

transparency, which is comparable to that of glass, makes it particularly well-suited for lenses, prisms, light guides, and windshields. Furthermore, the biocompatibility and dimensional stability of PMMA have also led to its widespread use in contact lenses, dental restorations and orthopedic implants.¹ The low density of PMMA (1.18 g cm⁻³) compared to that of alternative materials

This is an open access article under the terms of the Creative Commons Attribution-NonCommercial License, which permits use, distribution and reproduction in any medium, provided the original work is properly cited and is not used for commercial purposes.

© 2023 The Authors. *Journal of Polymer Science* published by Wiley Periodicals LLC.

¹Department of Chemistry, Clemson University, Clemson, South Carolina, USA

²Department of Materials Science and Engineering, Clemson University, Clemson, South Carolina, USA

SCHEME 1 General scheme for S—C bond-forming reactions by inverse vulcanization mechanisms.

like optical glass (with a density of 2.5 g cm⁻³) makes it an attractive alternative material for use in automotive components, given that reduced vehicle weight improves fuel efficiency and, consequently, reduces net carbon emissions. Despite the potential for improving sustainability in this regard, post-consumer PMMA is a persistent environmental pollutant.²⁻⁶

Currently PMMA is produced at 3.9 million metric tons per year, and only 10% of generated polymeric products is recycled. The majority of waste PMMA is incinerated or ends up in landfills. The routes currently used to recycle PMMA can be broadly divided into two categories: mechanical recycling and chemical recycling. Chemical recycling can be undertaken by several common processes such as gasification, thermal cracking, catalytic cracking and solvolysis. Despite the lower operating temperatures of some of the other processes, the thermal cracking of the waste PMMA in the absence of oxygen remains the most exploited process of PMMA depolymerization and recovery.

Elemental sulfur is a versatile component of plastic recycling/upcycling in a processes sometimes referred to as thiocracking. ^{10–12} Because elemental sulfur itself is a significantly underutilized by-product of fossil fuel refining, its use in materials also contributes positively to sustainability. ^{13–15}

At STP, elemental sulfur exists as α -sulfur, a crystalline allotrope of orthorhombic cyclo- S_8 . When cyclo- S_8 is heated above 159°C, cyclo- S_8 undergoes homolytic ring opening and self-polymerization to give polymeric sulfur diradicals of the form 'S—S_n—S' (Scheme 1).¹⁶ These sulfur-centered radicals can react with a range of organic species to facilitate the modification or disintegration of plastics. One such mechanism is inverse vulcanization, an S—C bond-forming reaction wherein sulfur-centered radicals add primarily to C—C π -bonds (Scheme 1).^{17,18} This process has been used to prepare a wide range of green composites derived from used cooking oil and greases, ^{19,20} biomass waste, ^{21–26} and other bio-olefins.

More recently, we devised a process to upcycle post-consumer poly(ethylene terephthalate) (PET, Scheme 2)¹¹ via a transesterification/inverse vulcanization mechanism. In this process, PET underwent transesterification with

Crosslinking in SPG

$$S_{X}$$
 S_{X}
 S_{X}

SCHEME 2 Upcycling of PET via transesterification/inverse vulcanization to give composite **SPG** having compressional and flexural strength exceeding those of ordinary Portland cement.

geraniol, an olefin-bearing, plant-derived terpenoid, followed by inverse vulcanization of the olefins to give a composite with high compressive strength that exceeds that of ordinary Portland cement (OPC). OPC production contributes ${\sim}8\%$ of all anthropogenic CO₂, 33 so finding alternatives such as geopolymer cements 34,35 or sulfur cements $^{36-42}$ will be important to achieve a sustainable economy.

Upcycling/recycling of waste plastic via the thiocracking strategy is attractive among potential routes because (1) it utilizes abundant sulfur by-product from fossil fuel refining, (2) produces materials whose mechanical structure is endowed with S—S bond networks, making them thermally recyclable, and (3) thiocracking takes place at lower temperatures than some routes to plastic recycling such as pyrolysis or thermal cracking, thus lowering the energy footprint.

26424169, 2024, 3, Downloaded from https://onlinelibrary.wiley.com/doi/10.1002/pol.20230609 by Clemson University, Wiley Online Library on [02/02/2024]. See the Terms and Conditions (https://onlinelibrary.wiley.com/term and-conditions) on Wiley Online Library for rules of use; OA articles are governed by the applicable Creative Commons License.

Given that tandem transesterification/inverse vulcanization could be achieved with ester functional groups in the PET backbone, we reasoned it would be similarly successful with pendant ester functional groups such as those found in PMMA. Herein we report a two-stage chemical recycling route to upcycle PMMA (Scheme 3). This process involves partial transesterification to substitute PMMA methyl with geranyl units, giving PGMA. The olefin-bearing geranyl sidechains in PGMA were then vulcanized by reaction of 10 wt.% PGMA with 90 wt.% elemental sulfur to yield a durable composite material (**PGMA-S**).

2 | RESULTS AND DISCUSSION

2.1 | Transesterification of PMMA with geraniol

The goal of this study was to upcycle PMMA via inverse vulcanization with sulfur. This goal requires olefin units to be installed on PMMA to participate in crosslinking via S-C bond-forming reactions via inverse vulcanization as shown in Scheme 1. To improve the sustainability of the chemistry, a plant-derived olefin-bearing terpenoid, geraniol, was selected for this purpose. The first step was transesterification of PMMA with geraniol to replace some of the methyl sidechains with geranyl groups (Scheme 3). The direct reaction of geraniol with PMMA was sluggish due to the steric hindrance to bringing the methyl ester and geraniol starting materials together for productive reaction in the geraniol versus methanol substitution equilibrium. Successful transesterification was, however, readily accomplished by adapting a procedure reported by Hawker's group for transesterification of PMMA with benzyl alcohol.⁴³ In this procedure, geraniol was deprotonated using lithium diisopropylamide (LDA) prior to its addition to PMMA. The resulting crude poly(geranyl methacrylate-*ran*-methyl methacrylate) (PGMA, Scheme 3) was isolated as a sticky solid by precipitation into an acidic water/methanol mixture. The pure material was obtained in 52% yield as a tan solid after Soxhlet extraction with methanol and drying in a vacuum oven at 60°C overnight.

PGMA was analyzed by ¹H nuclear magnetic resonance (NMR) spectrometry (Figure 1, full spectrum provided as Figure S1 in the SI). By comparing integration values for the geraniol-derived methylene proton signals (highlighted in green in Figure 1) to that of the methyl ester proton signal (highlighted in blue in Figure 1), the percent of methyl esters converted to geranyl esters was calculated to be 33%, corresponding to an olefin content of 14.2 mmol g^{-1} . The substitution of geranyl moieties for 33% of the methyl groups leads to a 1.4-fold increase in the average molecular weight per repeat unit in PGMA (140 g/mol) versus in the PMMA starting material (100 g/mol). GPC analysis of the PMMA starting material ($M_{\rm n} = 7700, M_{\rm w} = 12,800, D = 1.7$) and PGMA $(M_{\rm n}=11,700,\,M_{\rm w}=17,900,\,D=1.5)$ revealed a number average molecular weight ratio of 1.5, the same within statistical error as the 1.4 ratio predicted from analysis of ¹H NMR data. The somewhat narrower dispersity of PGMA (D = 1.5) versus that of PMMA (D = 1.7) is attributable to purification of PGMA by precipitation, which removed some lower molecular weight fractions.

The Fourier-transform infrared (FTIR) spectrum of PGMA (Figure 2) provided additional evidence for geraniol substitution. The FT-IR spectrum of geraniol has a distinctive broad O—H stretch in the range of 3300–3400 cm⁻¹, whereas the spectrum for PGMA showed no sign of a band attributable to an O—H stretch. The spectrum of PGMA also provided evidence for olefin incorporation by the appearance of an alkene C—H bending peaks at 840 cm⁻¹ and a C=C stretching peak at 1670 cm⁻¹. PGMA also retained characteristic features for ester functionalities in the form of the C=O stretch at 1724 cm⁻¹ and C—O stretch at 1145 cm⁻¹.

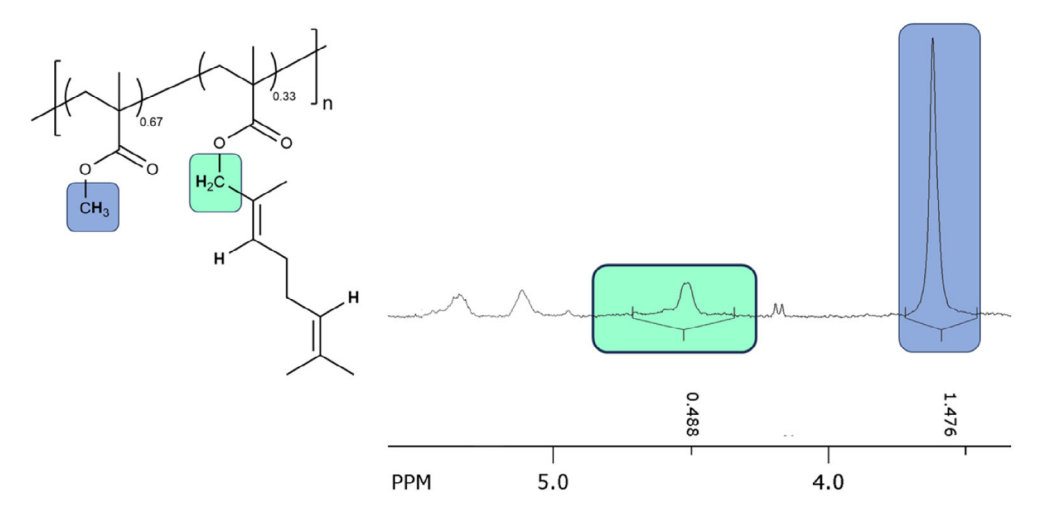
2.2 | Inverse vulcanization of PGMA to give PGMA-S

The second step in the proposed PMMA upcycling process was crosslinking olefin units in PGMA via inverse

SCHEME 3 Synthetic routes to PGMA and **PGMA-S**.

26424169, 2024, 3, Downloaded from https://onlinelibrary.wiley.com/doi/10.1002/pol.20230609 by Clemson University, Wiley Online Library on [02/02/2024]. See the Terms and Conditions (https://onlinelibrary.wiley.com/terms

-and-conditions) on Wiley Online Library for rules of use; OA articles are governed by the applicable Creative Commons License



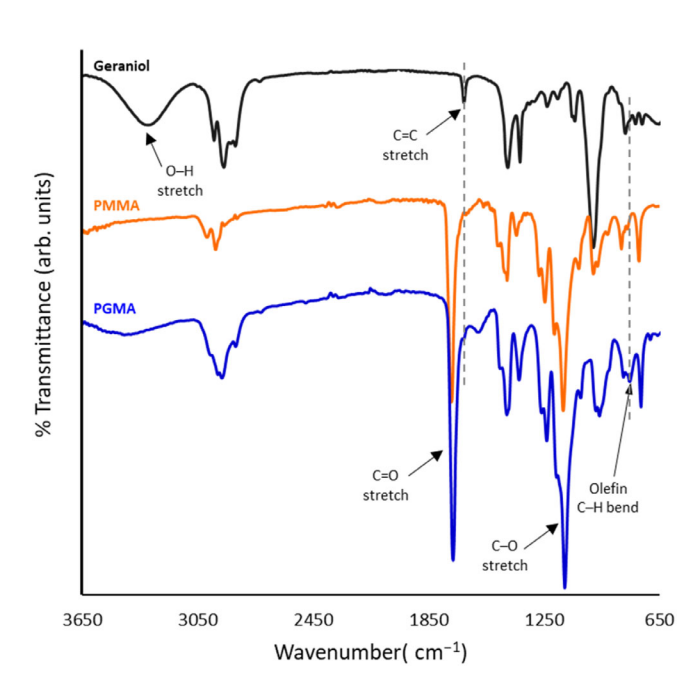
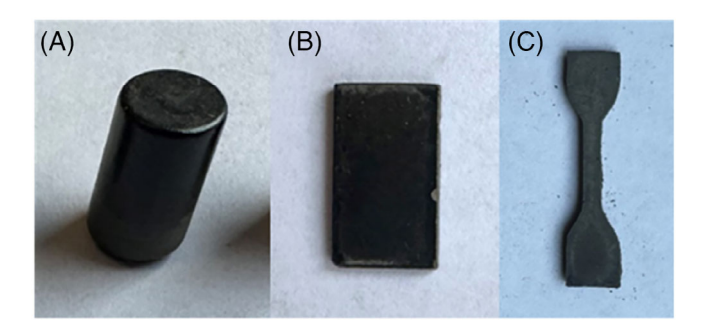


FIGURE 2 Fourier-transform infrared spectroscopy (FT-IR) traces for PGMA (blue trace) compared to those of PMMA (orange trace) and geraniol (black trace).

vulcanization. PGMA (10 wt.%) and 90 wt.% sulfur were thus reacted in a sealed pressure reactor under nitrogen. This reaction produced a homogeneous black liquid that became a glassy black solid (PGMA-S) when cooled to room temperature. Polymeric sulfur with no added organic material is very dark red in color above 159°C and becomes near black at higher temperatures even under inert atmosphere as the polymeric chains break into a mixture of oligomers.¹⁶ A mixture of oligosulfur crosslinking chains is similarly proposed as contributing to the dark color in the current material. The material was readily remeltable at 180°C and could be poured into silicone molds to give different shapes such as cylinders, rectangular prisms and dog bones to test compressive



Photos of **PGMA-S** that have been shaped into various shapes appropriate for compressive (A), flexural (B) and tensile (C) strength analysis.

strength, flexural strength, and tensile strength, respectively (Figure 3). The thermal reversibility of dynamic S-S covalent bond formation makes this polymer thermally recyclable,44 and no difference was observed in mechanical properties (vide infra) regardless of the number of melt/cast cycles (up to at least six cycles). Sulfur-sulfur bonds in oligosulfur crosslinking chains are less stable than those in S₈ rings, and so their homolytic cleavage occurs at temperatures of 159°C or below.16

High sulfur-content materials (HSMs) like PGMA-S are generally composites in which the sulfur is present in different forms. Toluene was used to extract sulfur species physically entrapped in but not covalently-bound to organic species within PGMA-S. The entrapped sulfur species, comprising 79 wt.% of the sample, are thought to be a mixture of species collectively known as "dark sulfur."45,46 Although the chemical identities of the individual species comprising dark sulfur are not fully understood, they are made almost entirely of sulfur atoms. In the current case, elemental microanalysis confirmed that the toluene soluble fractions of PGMA-S are >98% sulfur. Following the extraction of dark sulfur, the remaining sulfur can be presumed to exist predominantly

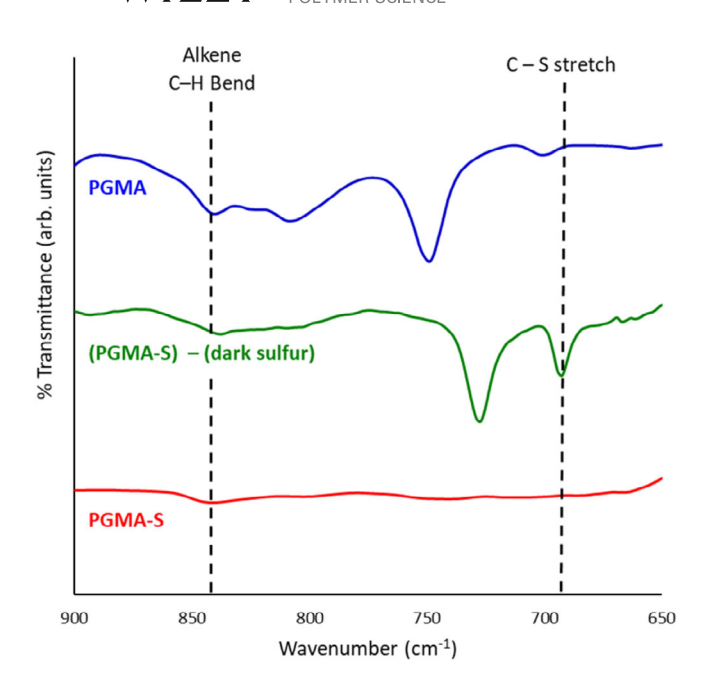


FIGURE 4 Portion of the FT-IR spectrum of **PGMA-S** (red trace) compared to that of PGMA (blue trace) and that of the toluene-insoluble (after extraction of dark sulfur) portion of **PGMA-S** (green trace).

in the crosslinking sulfur catenates represented as " $-S_x$ " in Scheme 3. The average value of x, known as the sulfur rank of a material, is often calculated for HSMs based on covalently linked sulfur content and olefin content (14.2 mmol g^{-1}). Recent studies on the mechanism of inverse vulcanization complicate this analysis. From the years 2013 to 2023, inverse vulcanization was thought to yield predominantly products of the form InV1 (Scheme 1)¹⁷ in which both olefinic carbons in the starting material participated in S—C bond formation. Recent work¹⁸ suggests that products of form **InV2**, wherein only one of the olefinic carbons participates in S-C bond-forming reactions, are not only observed but may even be the major product of inverse vulcanization reactions in some cases. Sulfur ranks for previously reported HSMs were calculated assuming products of the form InV1. When this assumption is made for PGMA-S, its sulfur rank is 20. This compares well to the sulfur ranks of other materials calculated using the same assumption. A sulfur rank of 22 was reported for GCS₉₀, a composite made from 90 wt.% sulfur and 10 wt.% geraniol-esterified cellulose, for example.⁴⁷ A significantly lower sulfur rank of 5 was reported for GPS, a composite made from 90 wt.% sulfur and 10 wt.% of esterified PET. 11 Sulfur ranks can be much higher, however. Some of the highest sulfur ranks reported for HSMs are for biomass-derived composites like PS₉₀, a composite of 90 wt.% sulfur/10 wt.% peanut shells, with a sulfur rank of 257. The olefin content of the peanut shells was very low in that

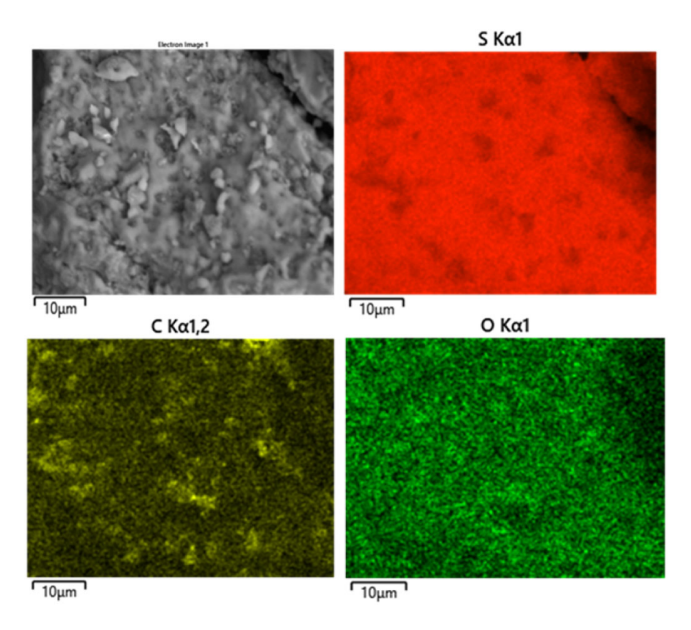


FIGURE 5 Scanning electron microscopy (SEM, gray image) with elemental mapping by energy dispersive X-ray analysis (EDX) of **PGMA-S**. Sulfur is shown in red, carbon in yellow, and oxygen in green.

case, however, so it would be expected to have more sulfur atoms available for crosslinking compared to **PGMA-S**.^{22,23}

To facilitate comparison to previously reported materials, the preceding comparison of sulfur ranks assumed InV1-like microstructures in PGMA-S. Considering recent mechanistic work, however, PGMA-S likely comprises a mixture of InV1- and InV2-type microstructures, in which case the sulfur rank in PGMA-S would be between 20 (if entirely InV1 product) and 40 (if entirely InV2 product). The actual sulfur ranks of previously reported HSMs made from olefins may likewise actually fall between the reported and twice the reported value if they were calculated using the assumption of entirely InV1 products.

A comparison of IR spectra for PGMA and **PGMA-S** (Figure 4) provides evidence for the consumption of alkenes in PGMA and the concomitant formation of S—C bonds. Because **PGMS-S** is 90 wt.% sulfur, its IR spectrum shows only weak signals attributable to organic units. As discussed above, however, a significant quantity of sulfur not involved in covalent bonds to C (i.e., dark sulfur) can be extracted from **PGMA-S** to leave a fraction with a higher concentration of organic material. The IR spectrum of the toluene-insoluble fraction (green trace in Figure 4) more clearly showed a prominent new peak at 692 cm⁻¹ attributable to the C—S stretch as evidence of the anticipated inverse vulcanization process.

Scanning electron microscopy (SEM) with elemental mapping by energy dispersive X-ray analysis (EDX) was

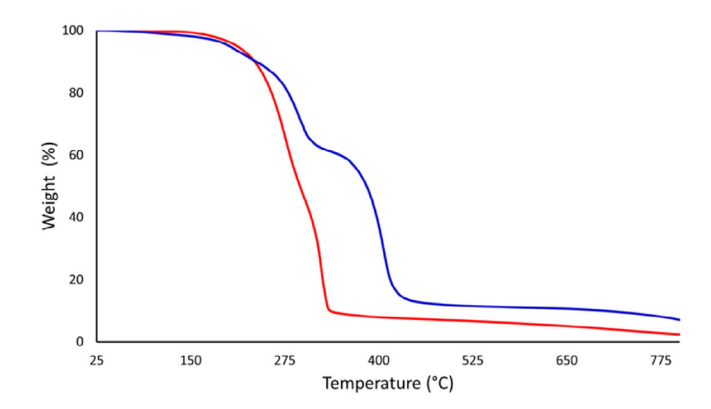


FIGURE 6 Thermogravimetric analysis (TGA) traces for PGMA (blue trace) and **PGMA-S** (red trace).

also used to assess the surface morphology of **PGMA-S** (Figure 5). Most of the surface of **PGMA-S** had a relatively uniform distribution of the elements carbon, oxygen and sulfur. Several areas (\sim 3 μ m wide on average) could be discerned in EDX images with a lower abundance of sulfur and higher concentration of carbon and oxygen. This indicates some separation of organic-rich from sulfur-rich domains on the micron scale despite their uniform appearance on the macroscale.

2.3 | Thermal and mechanical properties

Thermogravimetric analysis (TGA, blue trace in Figure 6) revealed a multistep decomposition of PGMA. The first decomposition step (201°C) is attributable to cleavage of ester bonds which gives low molecular fragments. The second (onset at 271°C) and third degradation (onset at 376°C) are attributable to chain scission of the terminal unsaturated groups and random scission within the polymer chain as are observed in unmodified PMMA.⁴⁸

TGA of **PGMA-S** as synthesized (containing both dark sulfur and covalently-linked $-S_x$ —) showed two distinct decomposition events (red trace in Figure 6). The initial event, leading to mass loss via sulfur sublimation and a T_d of at 211°C, is typical of HSMs and similar to that of *cyclo-S*₈ itself (229°C, Table 1). A less apparent mass loss feature attributable to degradation of the organic polymer portion contributed by PGMA-S was observed at 322°C.

Thermal morphological transitions of PGMA and **PGMA-S** were analyzed by differential scanning calorimetry (DSC, Figures S2 and S3 in the SI). DSC Analysis of PGMA by revealed a broad glass transition temperature ($T_{\rm g}$) centered at -11° C, but no melting temperature ($T_{\rm m}$) observed from -60 to 140° C.

The DSC thermogram for **PGMA-S** (Figure S3 in the SI) showed an endothermic phase transition appearing at

 $111^{\circ}C$ correspond to phase change from the orthorhombic to the monoclinic allotrope of S_8 and an endothermic transition at $117^{\circ}C$ attributable to the melting of monoclinic sulfur in sulfur-rich domains of the composite. A glass transition temperature was not observed in the range of -60 to $140^{\circ}C$ for PGMA-S, but a cold crystallization peak at $66^{\circ}C$ was observed corresponding to partial organization of the polymer chains.

The melting and cold crystallization enthalpies determined from the DSC analysis (Table 1) were used to calculate the percent crystallinity of the **PGMA-S** composite relative to crystalline orthorhombic sulfur. The percent crystallinity of the **PGMA-S** was found to be 51% which is comparatively higher than previous HSMs comprising 90 wt.% sulfur such as **SunBG90** (5 wt.% animal fat/5 wt.% sunflower oil) with 21% crystallinity²⁰ and **mPES** (10 wt.% PET derivatives) with 34% crystallinity.¹² A recent study suggests that composites with lower organic comonomer incorporation have higher crystallinities.²⁰

One of the goals of this study was to assess the extent to which the mechanical properties of PGMA-S could make it competitive with traditional building materials like ordinary Portland cement (OPC). OPC for housing foundations have flexural strengths of >3 MPa and require compressive strengths of ≥17 MPa (ACI specification 332.1R-06). Flexural strength tests of rectangular prisms of **PGMA-S** (Figure 3B) were conducted in single cantilever mode at room temperature (Table 2; stress-strain plot provided in Figure S4 of the SI). These tests showed that **PGMA-S** had a flexural strength of 4.76 MPa, exceeding that of OPC. The flexural strength of PGMA-S is comparable to that of several other HSMs comprising 90 wt.% S, including PS₉₀ (10 wt % unmodified peanut shells)²³ with a flexural strength of 4.8 MPa), GCS₉₀ (10 wt.% geraniolesterified cellulose)⁴⁷ with a flexural strength of 4.9 MPa, and **BAS₉₀** (10 wt.% 2,2',5,5'-tetrabromobisphenol A)⁴⁹ having a flexural strength of 4.7 MPa.

Mechanical test stand analysis of PGMA-S cylinders (Figure 3A) was used to determine compressive strength (Table 2; stress-strain plot provided in Figure S5 of the SI). The compressive strength of PGMA-S was 17.5 MPa, similar to the minimum compressive strength required for building foundations (17 MPa according to American Concrete Institute Guide to Residential Concrete Construction code ACI 332.1R-06). The compressive strength of PGMA-S lies in the middle of the range of compressive strengths observed for other HSMs (Table 2). Some composites having similar compressive strengths to that of PGMA-S are mAPS₉₅ (made from 95 wt.% sulfur and 5 wt.% allylated peanut, compressive strength = 17.1 MPa),²³ AA₉₅ (made from 95 wt.% sulfur and 5 wt.% allylated lignocellulosic biomass, compressive strength = 17.1 MPa),²² and **SunS** (made from

TABLE 1 Thermal and solubility parameters for PGMA, PGMA-S and cyclo-S₈.

Materials	$T_d/^{\circ} extbf{C}^{ extbf{a}}$	$T_m/^{\circ}$ C ^b	$T_{\infty-eta}/^{\circ}\mathbf{C^c}$	$T_{g,DSC}^{}$	Cold crystallization peaks/°C	$\Delta H_{ m m}$ J/g	$\Delta H_{ m cc}$ J/g	Percent crystallinity ^e	Percent insoluble fraction ^f
PGMA-S	211	117	111	NA	66	32	-36	51	21
Cyclo-S ₈	229	118	NA	NA	NA	45	NA	100	0

^aThe temperature at which the 5% mass loss was observed.

TABLE 2 Comparison of mechanical properties of **PGMA-S** to a range of chemically-related HSMs and to familiar ordinary Portland cement.

Materials	Compressive strength (MPa)	Flexural strength/ modulus (MPa)	Ultimate tensile strength at break (MPa)	Elongation at break (%)	Sulfur rank ⁿ
PGMA-S	17.5 ± 2.8	4.76/642	3.88 ± 1.20	26 ± 8	20
mAPS ₉₅ ^a	17.1 ± 0.0	5.6/1410	ND	ND	33
AA_{95}^{b}	17.1	ND	ND	ND	ND
SunS ^c	17.9 ± 3.1	ND	ND	ND	ND
PS ₉₀ ^d	21.3 ± 1.2	4.8/950	ND	ND	257
mPES ^e	26.9 ± 0.6	7.7/320	0.21 ± 0.04	<1	62
SunBG ₉₀ ^f	35.9 ± 0.7	7.7/460	ND	ND	54
R-BPA ₈₀ ^g	ND	ND	3.0 ± 0.4	32 ± 4	ND
GS ₉₀ ^h	ND	ND	1.16 ± 0.53	4.3 ± 1.8	ND
GS_{80}^{i}	ND	ND	2.32 ± 0.02	10.9 ± 2.1	ND
GCS ₉₀ ^j	ND	>4.9/950	ND	ND	22
BAS ₉₀ ^k	ND	>4.7/290	ND	ND	6
S-DCPD- EGDMA ^l	ND ^m	5–5.5	1.5–2	2.5–3	ND
Portland cement	17.0	3.7/580	ND	ND	NA

^aComposite made from 95 wt.% sulfur and 5 wt.% allylated peanut shells.

90 wt.% sulfur and 10 wt.% sunflower oil, compressive strength = 17.9 MPa). 50

In addition to its competitive compressive strength, **PGMA-S** was impervious to water absorption within the

detection limit after being submerged in deionized water for 24 h at room temperature. The high water absorption by mineral cements (up to 28 wt.%) plays a significant role in their mechanical failure, 51,52 so the low water

^bThe temperature at the peak maximum of the endothermic melting from the third heating cycle.

^cThe temperature at which the phase changes from orthorhombic to the monoclinic allotrope of S₈ occurs.

^dGlass transition temperature.

^eThe reduction of percent crystallinity of each sample was calculated with respect to sulfur (normalized to 100%).

^fPercent of non-extractable sulfur in each sample after toluene extraction.

^bComposite made from 95 wt.% sulfur and 5 wt.% allyl cellulose: allyl lignin blend.

 $^{^{\}rm c}$ Composite made from 90 wt.% sulfur and 10 wt.% sunflower oil.

^dComposite made from 90 wt.% sulfur and 10 wt.% unmodified peanut shells.

^eComposite made from 90 wt.% sulfur and 10 wt.% esterified PET.

^fComposite made from 90 wt.% sulfur, 5 wt.% brown grease and 5 wt.% sunflower oil.

^gComposite made from 80 wt.% sulfur and 20 wt.% O,O'-diallyl-2,2',5,5'-tetrabromobisphenol A.

^hComposite made from 90 wt.% sulfur and 10 wt.% guaiacol.

 $^{^{\}rm i}$ Composite made from 80 wt.% sulfur and 20 wt.% guaiacol.

^jComposite made from 90 wt.% sulfur and 10 wt.% of the esterified oxidized cellulose with geraniol.

^kComposite made from 90 wt.% sulfur and 10 wt.% 2,2',5,5'-tetrabromo(bisphenol A).

 $^{^{1}\!}Composite\ made\ from\ 50\ wt.\%\ sulfur\ loading,\ and\ 25\ wt.\%\ loading\ each\ of\ dicyclopentadiene\ and\ ethylene\ glycol\ dimethylacrylate.$

^mCompressive strength was not recorded but compression modulus was recorded.

ⁿValues reported assume **InV**1 type products as shown in Scheme 1.

26424619, 2024, 3, Downloaded from https://onlinelibtary.wiely.com/doi/10.1002/pol.20230609 by Clemson University, Wiley Online Library on [0202024]. See the Terms and Conditions (https://onlinelibrary.wiley.com/terms-and-conditions) on Wiley Online Library for rules of use; OA articles are governed by the applicable Creative Commons Licenses

uptake of **PGMA-S** makes it a good candidate for enhanced weathering durability.

The ultimate tensile strength at break (UTS) and elongation at break for PGMA-S were measured for dog bone-shaped specimens (Figure 3C). These tests reveal UTS of 3.88 MPa and elongation at break of 26%. PGMA-S thus exhibited higher UTS and elongation at break than most other HSMs (Table 2; stress-strain plot provided in Figure S6 of the SI). Another HSM made from waste plastic, mPES (a composite made from 90 wt.% sulfur and 10 wt.% esterified PET), 11 for example, had a UTS of only 0.21 MPa. Guaiacol-derived GS₉₀ (made from 90 wt.% sulfur and 10 wt.% guaiacol, UTS = 1.16 MPa) and GS_{80} (80 wt.% sulfur and 20 wt.% guaiacol, UTS of 2.32 MPa)²⁴ as well as **R-BPA₈₀** (comprising 80 wt.% sulfur and 20 wt.% O,O'-diallyl-2,2',5,5'tetrabromobisphenol A, UTS = 3.0 MPa), 38 had better tensile strength but still fall short of PGMA-S. A more detailed study on the effect of composition on tensile properties was carried out on terpolymers made from sulfur, ethylene glycol dimethylacrylate and dicyclopentadiene.⁵³ These terpolymers (S-DCPD-EGDMA in Table 2) exhibited better flexural strength between (5-5.5 MPa) but lower UTS (1.5-2 MPa) than PGMA-S. The high tensile strength of **PGMA-S** compared to the majority of HSMs may derive from its organic precursor being polymeric, whereas the other HSMs discussed above employ small molecular olefins as comonomers with sulfur.

3 | CONCLUSIONS

In conclusion, this study presents a strategy for conversion of commodity Poly (methyl methacrylate) into value-added materials. The bio-olefin, replaced the methyl ester group in PMMA to produce the random polymer, poly (methyl methacrylateran-geranyl methacrylate) with novel properties. This modification facilitated the cross-linking with polymeric sulfur chains which resulted in the formation of an organosulfur composite. PGMA-S exhibits remeltability and excellent recyclability. The material demonstrated a mechanical strength on par with commercial Portland cement. Also, the flexural strength of PGMA-S exceeded that of OPC. PGMA-S is expected to find promising applications in sustainable building materials due to its remarkable mechanical properties. Moving forward, the improvement of properties of the composite and development of improved synthetic methods holds the key to manufacturing advance sustainable commercially viable polymeric materials.

4 | EXPERIMENTAL

4.1 | Materials

Geraniol (Alfa Aesar), PMMA (Sigma Aldrich; $M_{\rm n}=7700,\,M_{\rm w}=12,\!800,\,D=1.7$), LDA (Sigma Aldrich, 2 M in THF/heptane/ethylbenzene) and sulfur (Dugas Diesel, USA) were used as received.

4.2 | General considerations

Fourier transform infrared spectra were obtained using a Shimadzu IR Affinity-1S instrument with an ATR attachment operating over 400–4000 cm⁻¹ at ambient temperature.

The proton NMR spectra were recorded on a Bruker NEO-300 MHz spectrometer at room temperature. Spin-Works 4.2.11 software was used to process obtained data.

Gel permeation chromatography (GPC) was carried out on a Shimadzu GPC using a Phenogel 5u 10E4A gel column and RID 10A detector and with tetrahydrofuran as an eluent at a flow rate of 1 mL min⁻¹. A set of polystyrene standards (obtained from Polymer Source, Inc.) from 136,269 to 7215 molecular weight was used to calibrate the GPC instrument. Data acquisitions were carried out with the Labsolutions GPC software.

Thermogravimetric analysis (TGA) data were recorded on a TA SDT Q600 instrument over the range $25-800^{\circ}$ C, with a heating rate of 10° C min⁻¹ under a flow of N₂ (20 mL min⁻¹).

Differential scanning calorimetry (DSC) data were acquired using a Mettler Toledo DSC 3 STARe System from -60 to 140° C, with a heating rate of 10° C min $^{-1}$ under a flow of N₂ (50 mL min $^{-1}$). Each DSC measurement was carried out over three heat-cool cycles, and data are reported for the third cycle.

Flexural strength analysis was performed using a Mettler Toledo DMA 1 STARe System in single cantilever mode. The samples were cast from silicone resin molds (Smooth-On Oomoo® 25 tin-cure). The sample dimensions were $1.5\times10\times18$ mm. Flexural analysis was performed in duplicate and results were averaged. The clamping force was 1 cN m.

Compressional and tensile analyses were performed on a Mark-10 ES30 test stand equipped with a M3-200 force gauge (1 kN maximum force with ± 1 N resolution). Compression cylinders were cast from silicone resin molds (Smooth-On Oomoo® 25 tin-cure) with diameters of ${\sim}6$ mm and heights of ${\sim}10$ mm. Samples were manually sanded to ensure uniform dimensions. Compressional analysis was performed in triplicate and the results were averaged.

SEM and EDX were acquired on a Schottky Field Emission Scanning Electron Microscope SU5000 operating in variable pressure mode with an accelerating voltage of 15 keV.

4.2.1 | Synthesis of PGMA

This procedure follows a reported procedure, but uses geraniol⁴³ in place of benzyl alcohol. Poly(methyl methacrylate) (8.01 g, 80.0 mmol) was placed in a round bottom flask and the flask was sealed with a rubber septum stopper. The sealed system was then purged with nitrogen and a dynamic nitrogen flow was maintained throughout the remainder of the experiment. After about 20 min of purging with nitrogen, a 160 mL aliquot of anhydrous N,N-dimethylformamide (DMF) was transferred to the sealed flask of PMMA via syringe. A separate three-neck round bottom flask was equipped with a Teflon-coated magnetic stir bar and a reflux condenser. Geraniol (12.3 g, 80.0 mmol) was added to the three-neck flask. The flask was then sealed with rubber septum stoppers and purged with nitrogen. Magnetic stirring was initiated and the flask was cooled in an ice bath. A 40.0 mL aliquot of a lithium diisopropylamide solution (LDA, 2 M solution in THF/heptane/ethylbenzene, 80.0 mmol) was added to the round bottom flask via a degassed syringe. Following complete addition of the LDA solution, the mixture was allowed to stir for an additional 30 min while the flask was maintained in an ice bath. After this time, the PMMA solution from the other flask was added dropwise to the rapidly stirring geraniol/LDA reaction mixture. Following addition, the ice bath was removed and the solution was stirred for 10 min before heating the mixture at 120°C for 2 h. After 2 h, the reaction mixture was poured into an acidic water methanol mixture (80 mL DI water: 80 mL methanol: 4 mL conc. HCl). Liquid-liquid extraction of the product into dichloromethane (200 mL) was undertaken and the organic fractions were collected. Volatiles were removed from the organic layer vacuum in a rotary evaporator. The remaining non-volatile organics were redissolved in dichloromethane (100 mL) and 100 mL of water was added. Phase separation was not efficient, so the mixture was centrifuged and the water layer was removed by pipet. This process was repeated five times to extract residual DMF. The crude polymer was a very sticky beige solid that was difficult to collect from glassware and centrifuge tube surfaces, so some loss of material occurred during these manipulations. Volatiles were again removed from the organic layer remaining after the final centrifugation. At this point, ¹H NMR spectroscopic analysis still showed the presence of some unreacted geraniol. Initial trials to remove geraniol by washing the solid with hexanes were unsuccessful. Residual geraniol was successfully removed by Soxhlet extraction with

methanol for 5 h, followed by drying the solid in a vacuum oven at 60°C overnight to give the product as a tan solid (5.82 g, 51.8%, NMR data provided in Figure S1, SI). Data from GPC: $M_{\rm n}=11,700, M_{\rm w}=17,900, D=1.5$.

4.2.2 | Synthesis of **PGMA-S**

CAUTION: Heating elemental sulfur with organics can result in the formation of H_2S gas. H_2S is toxic, foul-smelling, and corrosive. A 13.50 g sample of elemental sulfur and 1.500 g of PGMA were added to a Parr bomb reactor. Mechanical stirring was started and the reactor was brought to 250°C over about 1 h and once this temperature was reached stirring was continued for 1 h. The reactor was allowed to cool to ambient temperature before opening it to reveal the product as a nearly black solid (recovered yield 12.65 g, 84.33%). Elemental analysis calculated: C, 7.08; S, 90.00; H, 1.03%. Found: C, 4.99; S, 94.08; H, 0.19%. (Atlantic Microlab, Inc.).

4.2.3 | Extraction of dark sulfur with toluene

A 0.1360 g sample of finely ground **PGMA-S** was used to perform toluene extractions. The finely ground material was stirred with 20 mL of toluene for about an hour. Then the solid was allowed to settle for 30 min & supernatant was pipetted off into a separate vial. After that another 20 mL of toluene was added. The residual toluene was evaporated and each vial was weighed to determine the mass of the insoluble fraction.

ACKNOWLEDGMENTS

We thank the National Science Foundation (CHE-2203669 to RCS) for financial support.

ORCID

Rhett C. Smith https://orcid.org/0000-0001-6087-8032

REFERENCES

- [1] U. Ali, K. J. B. A. Karim, N. A. Buang, Polym. Rev. 2015, 55, 678.
- [2] A. Ogura, Purasuchikkusu 2022, 73, 41.
- [3] T. Zhao, L. Tan, X. Han, X. Wang, Y. Zhang, X. Ma, K. Lin, R. Wang, Z. Ni, J. Wang, J. Wang, Sci. Total Environ. 2022, 804, 150252.
- [4] C. Venancio, I. Melnic, M. Tamayo-Belda, M. Oliveira, M. A. Martins, I. Lopes, Sci. Total Environ. 2022, 806, 150491.
- [5] X.-X. Zhou, S. He, Y. Gao, H.-Y. Chi, D.-J. Wang, Z.-C. Li, B. Yan, Environ. Sci. Technol. 2021, 55, 3032.
- [6] I. Brandts, C. Barria, M. A. Martins, L. Franco-Martinez, A. Barreto, A. Tvarijonaviciute, L. Tort, M. Oliveira, M. Teles, J. Hazard. Mater. 2021, 403, 123590.

26424169, 2024, 3, Downloaded from https://onlinelibrary.wiley.com/doi/10.1002/pol.20230609 by Clemson University, Wiley Online Library on [02/02/2024]. See the Terms

Wiley Online Library for rules of use; OA articles

are governed by the applicable Creative Commons

- [7] M. Sponchioni, S. Altinok, in *Advances in Chemical Engineering* (Eds: D. Moscatelli, M. Pelucchi), Academic Press, Cambridge, MA 2022, p. 269.
- [8] J. De Tommaso, J.-L. Dubois, *Polymer* 2021, 13, 2724. https://doi.org/10.3390/polym13162724
- [9] E. Esmizadeh, S. Khalili, A. Vahidifar, G. Naderi, C. Dubois, in *Handbook of Ecomaterials* (Eds: L. M. T. Martínez, O. V. Kharissova, B. I. Kharisov), Springer International Publishing, Cham 2018, p. 1.
- [10] T. Thiounn, M. S. Karunarathna, M. K. Lauer, A. G. Tennyson, R. C. Smith, *RSC Sustain*. **2023**, *1*, 535.
- [11] C. P. Maladeniya, A. G. Tennyson, R. C. Smith, J. Polym. Sci. 2023, 61, 787.
- [12] C. V. Lopez, R. C. Smith, Mater. Adv. 2023, 4, 2785.
- [13] X. Zhang, Y. Tang, S. Qu, J. Da, Z. Hao, ACS Catal. 2015, 5, 1053.
- [14] A. Demirbas, H. Alidrisi, M. A. Balubaid, Pet. Sci. Technol. 2015, 33, 93.
- [15] G. Kutney, Sulfur. History, Technology, Applications & Industry, Toronto, ChemTec 2007.
- [16] B. Meyer, Chem. Rev. 1964, 64, 429.
- [17] W. J. Chung, J. J. Griebel, E. T. Kim, H. Yoon, A. G. Simmonds, H. J. Ji, P. T. Dirlam, R. S. Glass, J. J. Wie, N. A. Nguyen, B. W. Guralnick, J. Park, A. Somogyi, P. Theato, M. E. Mackay, Y.-E. Sung, K. Char, J. Pyun, *Nat. Chem.* 2013, 5, 518.
- [18] J. Bao, K. P. Martin, E. Cho, K.-S. Kang, R. S. Glass, V. Coropceanu, J.-L. Bredas, W. O. N. Parker Jr., J. T. Njardarson, J. Pyun, J. Am. Chem. Soc. 2023, 145, 12386.
- [19] M. J. H. Worthington, R. L. Kucera, I. S. Albuquerque, C. T. Gibson, A. Sibley, A. D. Slattery, J. A. Campbell, S. F. K. Alboaiji, K. A. Muller, J. Young, N. Adamson, J. R. Gascooke, D. Jampaiah, Y. M. Sabri, S. K. Bhargava, S. J. Ippolito, D. A. Lewis, J. S. Quinton, A. V. Ellis, A. Johs, G. J. L. Bernardes, J. M. Chalker, *Chem. Eur. J.* 2017, 23, 16219.
- [20] C. V. Lopez, A. D. Smith, R. C. Smith, RSC Adv. 2022, 12, 1535
- [21] M. S. Karunarathna, C. P. Maladeniya, M. K. Lauer, A. G. Tennyson, R. C. Smith, *RSC Adv.* 2023, *13*, 3234.
- [22] M. K. Lauer, M. S. Karunarathna, A. G. Tennyson, R. C. Smith, *Mater. Adv.* **2020**, *1*, 590.
- [23] M. K. Lauer, M. S. Karunarathna, A. G. Tennyson, R. C. Smith, *Mater. Adv.* **2020**, *1*, 2271.
- [24] M. S. Karunarathna, M. K. Lauer, R. C. Smith, J. Mater. Chem. A 2020, 8, 20318.
- [25] M. K. Lauer, T. A. Estrada-Mendoza, C. D. McMillen, G. Chumanov, A. G. Tennyson, R. C. Smith, Adv. Sustain. Syst. 2019, 3, 1900062.
- [26] M. S. Karunarathna, M. K. Lauer, T. Thiounn, R. C. Smith, A. G. Tennyson, J. Mater. Chem. A 2019, 7, 15683.
- [27] A. Hoefling, D. T. Nguyen, Y. J. Lee, S.-W. Song, P. Theato, Mater. Chem. Front. 2017, 1, 1818.
- [28] A. Hoefling, Y. J. Lee, P. Theato, Macromol. Chem. Phys. 2017, 218, 1600303.
- [29] A. E. Davis, K. B. Sayer, C. L. Jenkins, *Polym. Chem.* 2022, 13, 4634.
- [30] C. Herrera, K. J. Ysinga, C. L. Jenkins, ACS Appl. Mater. Interfaces 2019, 11, 35312.
- [31] C. P. Maladeniya, R. C. Smith, J. Compos. Sci. 2021, 5, 257.

- [32] C. P. Maladeniya, M. S. Karunarathna, M. K. Lauer, C. V. Lopez, T. Thiounn, R. C. Smith, Mater. Adv. 2020, 1, 1665.
- [33] L. K. Turner, F. G. Collins, Constr. Build. Mater. 2013, 43, 125.
- [34] G. Furtos, L. Molnar, L. Silaghi-Dumitrescu, P. Pascuta, K. Korniejenko, J. Nat. Fibers 2022, 19, 6676.
- [35] G. Furtos, L. Silaghi-Dumitrescu, P. Pascuta, C. Sarosi, K. Korniejenko, J. Nat. Fibers 2021, 18, 285.
- [36] B. Gutarowska, M. Piotrowska, A. Kozirog, J. Berlowska, P. Dziugan, R. Kotynia, D. Bielinski, R. Anyszka, J. Wreczycki, *Materials* 2019, 12, 2602.
- [37] E. D. Weil, Phosphorus Sulfur Silicon Relat Elem 1991, 59, 325.
- [38] T. Thiounn, M. S. Karunarathna, L. M. Slann, M. K. Lauer, R. C. Smith, J. Polym. Sci. 2020, 58, 2943.
- [39] T. Thiounn, A. G. Tennyson, R. C. Smith, RSC Adv. 2019, 9, 31460.
- [40] R. Gregor, A. Hackl, Adv. Chem. Ser. 1978, 165, 54.
- [41] N. G. Shrive, J. E. Gillott, I. J. Jordaan, R. E. Loov, ACS Symp. Ser. 1982, 183, 137.
- [42] H. A. Okumura, Concr. Int. 1998, 20, 72.
- [43] C. Fleischmann, A. Anastasaki, W. R. Gutekunst, A. J. McGrath, P. D. Hustad, P. G. Clark, D. S. Laitar, C. J. Hawker, J. Polym. Sci., Part A: Polym. Chem. 2017, 55, 1566.
- [44] S. J. Tonkin, C. T. Gibson, J. A. Campbell, D. A. Lewis, A. Karton, T. Hasell, J. M. Chalker, *Chem. Sci.* 2020, 11, 5537.
- [45] J. J. Dale, J. Stanley, R. A. Dop, G. Chronowska-Bojczuk, A. J. Fielding, D. R. Neill, T. Hasell, Eur. Polym. J. 2023, 195, 112198.
- [46] J. J. Dale, S. Petcher, T. Hasell, ACS Appl. Polym. Mater. 2022, 4, 3169.
- [47] M. K. Lauer, A. G. Tennyson, R. C. Smith, ACS Appl. Polym. Mater. 2020, 2, 3761.
- [48] T. Kashiwagi, A. Inaba, J. E. Brown, K. Hatada, T. Kitayama, E. Masuda, *Macromolecules* 1986, 19, 2160.
- [49] T. Thiounn, M. K. Lauer, M. S. Karunarathna, A. G. Tennyson, R. C. Smith, SusChem 2020, 1, 183.
- [50] C. V. Lopez, M. S. Karunarathna, M. K. Lauer, C. P. Maladeniya, T. Thiounn, E. D. Ackley, R. C. Smith, J. Polym. Sci. 2020, 58, 2259.
- [51] L. Basheer, J. Kropp, D. J. Cleland, Constr. Build. Mater. 2001, 15, 93.
- [52] N. Z. Muhammad, A. Keyvanfar, M. Z. A. Majid, A. Shafaghat, J. Mirza, Constr. Build. Mater. 2015, 101, 80.
- [53] J. A. Smith, S. J. Green, S. Petcher, D. J. Parker, B. Zhang, M. J. H. Worthington, X. Wu, C. A. Kelly, T. Baker, C. T. Gibson, J. A. Campbell, D. A. Lewis, M. J. Jenkins, H. Willcock, J. M. Chalker, T. Hasell, *Chem.—Eur. J.* 2019, 25, 10433.

SUPPORTING INFORMATION

Additional supporting information can be found online in the Supporting Information section at the end of this article.

How to cite this article: S. K. Wijeyatunga, K. M. Derr, C. P. Maladeniya, P. Y. Sauceda-Oloño, A. G. Tennyson, R. C. Smith, *J. Polym. Sci.* **2024**, *62*(3), 554. https://doi.org/10.1002/pol.20230609